Dihoru, L., Crewe, A., Liu, Z., & Taylor, C. (2018). Shaking table studies of FRP-reinforced masonry: experimental and numerical results. In *Proceedings of the 16th European Conference on Earthquake Engineering* (Geotechnical, Geological, and Earthquake Engineering; Vol. 46, No. 1). http://www.16ecee.org/proceedings

Peer reviewed version

Link to publication record in Explore Bristol Research
PDF-document

University of Bristol - Explore Bristol Research
General rights

SHAKING TABLE STUDIES OF FRP-REINFORCED MASONRY: EXPERIMENTAL STUDIES AND NUMERICAL RESULTS

Luiza DIHORU[1], Adam J. CREWE[2], Zhen LIU[3], Colin A. TAYLOR[4]

ABSTRACT

Numerous investigations to date have explored the potential use of FRP (Fibre Reinforced Polymers) on concrete and on masonry structures as a strengthening solution. The majority of these studies have focused on the in-plane or the out-of-plane monotonic loading and the general trend has been to adapt the monotonic loading assessment methods for seismic loading as well. A need to evaluate the mechanical behaviour of the FRP reinforced masonry infill panels under truly seismic conditions has emerged. Full-scale shaking table tests were carried out at the University of Bristol on both reinforced and unreinforced masonry specimens in order to fill the gap in the existing knowledge on the dynamic behaviour of these structures. This paper presents a summary of the experimental programme together with the most relevant findings from tests. The experimental observations on pre-cracking and post-cracking behaviour are meant to provide more understanding on the reinforcement requirements associated with a seismically-sound system. Two modelling techniques have been used to model the behaviour of the FRP strengthened wall. Firstly, a neural network based software tool and secondly, a discrete element based model have been used to predict the mechanical response of FRP strengthened masonry walls and the simulation outcomes have been compared with the experimental ones.

Keywords: masonry; infill panel; FRP-reinforcement; neural networks; discrete element

1. INTRODUCTION

A large number of buildings in Europe today are unreinforced masonry (URM) buildings that were designed with little or no regard for seismic resilience. Masonry is brittle in nature, hence particularly sensitive to out-of-plane and in-plane loading. Conventional retrofitting methods for existing masonry structures include the addition of framing elements (e.g. steel columns, steel beams) or the strengthening of the surface via surface treatments (e.g. addition of shotcrete or ferrocement) (Gilstrap and Dolan 1998).

Recent years have seen proposals and practical applications that use fibre reinforced polymers (FRP) materials as strengthening alternative for URM structures. The rationale for using FRP on masonry structures has been investigated by many researchers in relation to the advantages and the disadvantages of the materials employed and their application methods. Factors like seismic risk, cost, functionality during and after retrofit and aesthetics were part of the evaluation criteria. The cost of strengthening, the possible alteration of functionality of the building, the increase of inertia and seismic forces by the addition of mass and the possible overloading of the existing foundation have been topical issues since the early '70s, when the FRPs started to spread beyond the niche applications in the aerospace and defence areas to become an increasingly cheaper option in the construction industry (Bakis et al. 2002).

The preferred method of reinforcement has been with FRP strips or continuous jackets applied on the

---

[1] Senior Research Associate, University of Bristol, Bristol, United Kingdom, luiza.dihoru@bristol.ac.uk

[2] Reader, University of Bristol, Bristol, United Kingdom, A.J.Crewe@bristol.ac.uk

[3] PhD Student, University of Bristol, Bristol, United Kingdom, zl15471@bristol.ac.uk

[4] Professor, University of Bristol, Bristol, United Kingdom, Colin.Taylor@bristol.ac.uk

masonry surface using a layer of epoxy-based resin. Detailed concepts on the effectiveness of the method were first developed by Triantafillou and Fardis (1993). In 1994, Schwegler (1994) reports the first results of a full-scale in-plane and out-of-plane cyclic testing of masonry walls reinforced with carbon fibre polymers. A large number of studies have focused since on the in-plane and/or the out-of-plane monotonic loading of reinforced masonry. Results from walls subjected to monotonic (Albert et al. 2001, Hamilton and Dolan 2001) and cyclic (Ehsani et al.1999, Kuzic et al. 2003) tests have demonstrated that the presence of the FRP increases the capacity of the panels and changes the crack patterns and failure modes. It has been shown that when out-of-plane bending dominates, horizontally applied strips of FRP may offer a considerable strength increase, while in the case of in-plane bending high reinforcement ratios placed near the highly stressed zones could offer the solution. The use of anchorage and clamping of the FRP strips to prevent end-peeling has also been addressed and many researchers have focused on special strengthening techniques which result in a more economical use of materials (Triantafillou et al 1992, Lamanna et al. 2001).

The main mechanisms of failure have been identified as being the FRP delamination in flexure, FRP delamination in shear, brick crushing and FRP rupture. The occurrence of these events has been shown to be largely dependent on the type of loading, the panel boundary conditions and the reinforcement layout. Ehsani et al (1999) reported on half-scale masonry walls reinforced with glass fibre fabrics and subjected to cyclic out-of-plane loading. Their findings show that the mode of failure is controlled by tensile failure when wider and lighter composite fabrics are used and by delamination when stronger ones are used. The specimens were capable of supporting a lateral load of 32 times the weight of the wall and deflected as much as 2% of the wall height. The arching of panels was observed when low reinforcement ratios were used and when the reinforced panel cracking pattern resembles more the one exhibited by the URM walls. Arching is reported as a main resistance mechanism in URM panels subjected to out-of-plane loads. Taylor (1998) carried out shaking table tests on thirteen URM specimens with various boundary conditions. The panels showed a highly non-linear behaviour dependent on the boundary conditions and the input motion. The shift of frequency response followed the panel's stiffness degradation under dynamic loading. The top and bottom supported panels cracked at table accelerations ranging between 0.33-1.89 g. A need to extend this investigation for FRP-reinforced masonry emerged.

Up to date, the out-of-plane response of URM or FRP-reinforced infill panels has been modelled using the flexural theory of masonry present in the building codes (Velasquez-Dimas *et. al.*, I and II, 2000, Hamilton and Dolan 2001), with the adaptation of the monotonic loading assessment methods for seismic loading as well. However, the developed analytical models have not been validated through dynamic experimentation. The present study, carried out by the University of Bristol (UOB), is meant to fill the gap in the knowledge and provide experimental inspiration for modellers. Full scale control infill panel specimens (URM) and FRP-reinforced ones were tested in monotonic and shaking table tests (Dihoru and Taylor 2006), in order to assess the trends in mechanical behaviour and to provide the relevant background for the initial assumptions in modelling. This paper presents the test programme and the main findings from the seismic testing activity. A neural network tool and a discrete element based model have been developed to probe the seismic response of both the URM and the reinforced panels and pave the way for future sensitivity studies.

2. EXPERIMENTAL PROGRAMME

2.1 Work Objectives

An experimental programme of testing was carried out in the Earthquake Engineering Research Laboratory (EERC) at the UOB in order to investigate the mechanical behaviour of URM and FRP-reinforced masonry infill panels. Although both the masonry and the FRP have a brittle type of failure, their combination was expected to show increased load-carrying capacity and ductility favoured by the elastic deformation of fibres and the shear transfer in the resin connection layer. Beside the strength benefits, a slowly-progressing mode of failure was pursued. The sudden collapse of unreinforced

masonry or the explosive failure of the FRP needed to be substituted by a slow and energy dissipative process that could be the FRP delamination. It was believed that the layout of the FRP and the reinforcement ratios could be used as control factors in triggering the failure mechanisms.

URM and FRP-reinforced infill panels were subjected to one-axis seismic tests on the EERC's shaking table, with the purpose of investigating the following aspects of mechanical response:

- mechanisms of the failure modes
- crack patterns and strain profiles
- influence of the FRP layout and reinforcement ratio on the mechanical response
- influence of the loading characteristics on the mechanical response
- evolution of panel stiffness and modal parameters under seismic loading

2.2 Materials and Specimen Configurations

Masonry Panels

The research concentrated on the simplest case of a panel supported at its top and bottom only, with the vertical sides being unrestrained. All specimens were single-wythe, top and bottom supported panels (size 3000mm x 2000mm x 100mm). The panels were built within a pin-jointed steel frame fabricated from 254mm x254mm universal column sections. The sections were stiffened by thick plates welded longitudinally between the flanges on both sides of the beams in order to prevent the flange flexure.

The specimens were built off the shaking table and left to cure using standard practices. Each masonry wall was built in two lifts and were top and bottom supported. Mortar was packed on the top side of the wall to fill the gap caused by shrinkage. The walls were left for 21 days to cure. When the specimens were cured, they were bolted down onto the shaking table and instrumented.

A summary of the URM material characteristics is given below:

- concrete facing bricks: acc. to BS6073, size: 215mm x102mm x 65mm, density: 2200 kg/m^3 (given by the manufacturer), compressive strength: 25 N/mm^2 (measured).
- mortar: general purpose mortar for masonry, corresponding to group III acc. to BS EN 998-2:2003, composition 1:1:6 (cement: lime: sand) (given by the manufacturer), compressive strength: 6 N/mm^2 (measured).
- masonry: max. compressive stress = 18 N/mm^2 (measured), max. tensile strain = 0.6 % (measured).

FRP Reinforcement

When selecting the FRP materials for reinforcement of panels, the main parameters that are generally taken into account are the specific strength (tensile strength/specific gravity) or the specific stiffness (modulus of elasticity/specific gravity). The carbon fibre (CF) composites exhibit better specific strength and specific stiffness values than their competitors. However, when the seismic behaviour of the retrofitted system comes into play, the systems' ductility and capacity of energy absorption become important. Fibre ductility is increasing from carbon to aramid and further to glass. After weighing the benefits and the disadvantages of a large set of FRP materials (both plates and wraps), a glass-fibre fabric system was selected for reinforcement (manufacturer: EXCHEM Ltd., UK). Its mechanical properties are given in Table 1. Three FRP-reinforced panels were built with the following reinforcement ratios (RR): 100 %, 60% and 40 % as shown in Figure 1. The FRP mounting procedure started with the preparation of masonry surface for primer application. Attention focused on cleaning the joints and on removing of excessive mortar from the wall surface. The surface was cleaned with a wire brush and was checked for tool marks and other surface variation problems. A dual system that could be used as a primer and as a laminating resin was employed (Selfix MPA 22 Laminating Resin from Exchem Ltd.). A foam roller was used to apply a thin layer of primer on the wall surface (average primer consumption 1kg/5m^2). The primer was used to close the existing porosity of the wall surface

and to provide a good bonding substrate for the resin. Pre-cut FRP strips of 300mm x 1960mm were saturated with resin (average resin consumption: $1kg/3m^2$) while lying on a horizontal surface. They were then applied to the wall surface using a foam roller and by applying hand-pressure. The change of fabric colour from white to transparent yellow was used as an indication that saturation was reached. A final layer of laminating resin was applied on the FRP fabric for full saturation, protection and instrumentation purposes. The reinforcement strips were applied to both faces of the panel. The reinforcement was applied to overlap the surrounding frame by at least 75mm, in order to prevent the panel detaching from the frame. The FRP fabric was mounted at 21 days after the building of the wall. The testing took place at min. 10 days after the FRP install. Figure 2 shows two FRP-reinforced panels before testing.

Table 1 FRP properties employed in the tests

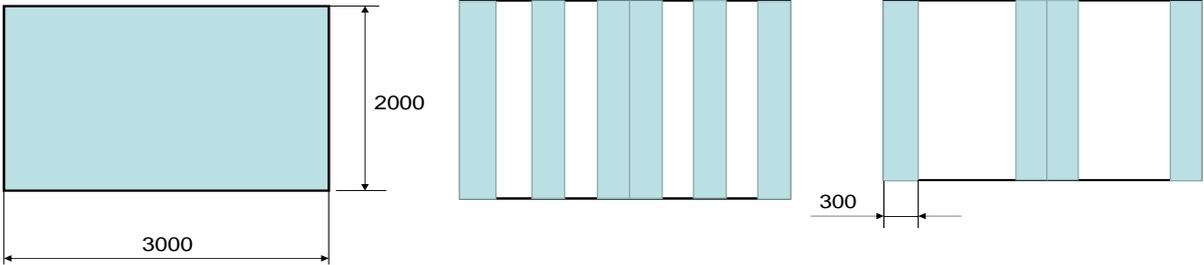| Fibre	Tensile strength (N/mm²) fibre/ laminate	Modulus of elasticity (kN/mm²) fibre/ laminate	Elongation (%)	Thickness (mm)	Weight (g/m²)
Glass Fibre Wrap Type E	3450 /1099	73 / 42	4.5	0.167	432

Figure 1 Layouts of FRP fabric on the masonry panel. Left: continuous jacket (100% RR), middle: vertical strips (60% RR), right: vertical strips (40% RR). Reinforcement applied on both sides of the panel. (Note: RR stands for Reinforcement Ratio).

Figure 2 FRP reinforced panel with 100% RR (left) and panel with 60% RR (right).

2.3 Instrumentation

A diagram showing the array of instruments deployed on the specimens is shown in Figure 3. Displacement transducers type Celesco PT101 were placed at midheight and at positions symmetrically-

located about the centreline on the wall to measure out-of-plane deflection. The body of the transducers were fixed to a rigid frame standing parallel to the wall surface. Four load cells were incorporated in the four bolts attaching the top beam to the frame columns. The load cells measured the arching forces on the wall. The top beam was separated from the top of the column by washers around the instrumented bolts. Vishay type CEA-06-250UW-350 strain gauges were employed to record the FRP tensile strain at midheight and at locations symmetrically located about the centreline of the wall. The strain gauges were mounted on the FRP fabric in areas located on top of a brick unit. All the strain gauges employed had uniaxial wiring. Accelerometers type Setra 141A were installed on the shaking table platform, on the wall panel and on the top beam to record acceleration during the seismic tests.
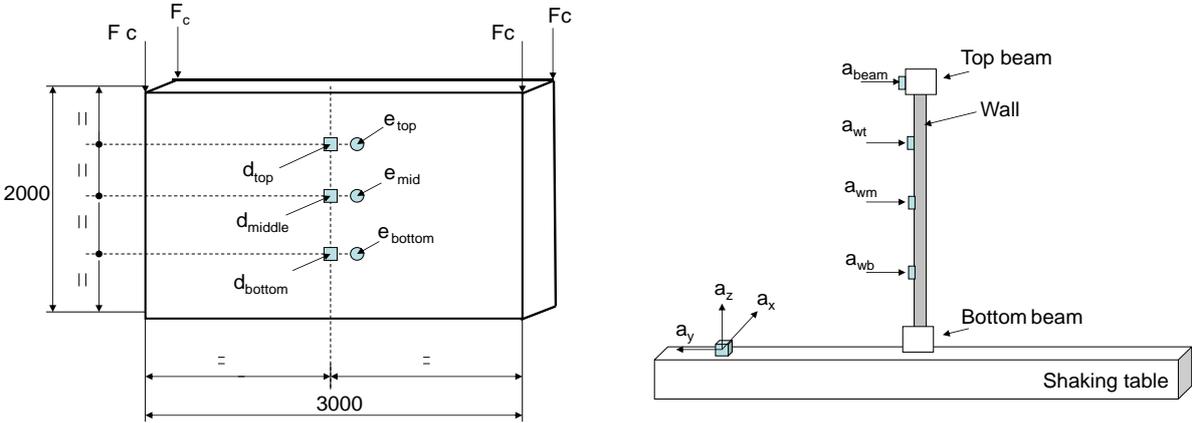

Figure 3 Instrumentation layout diagram. Left: panel front view showing displacement transducers, strain gauges 41and load cell positions. Right: panel side view showing accelerometers on the wall and on the shaking table platform.

2.4 Seismic Inputs

The applied seismic inputs were based on an elastic response spectrum for Soil B according to Eurocode 8. The design response spectrum is presented in Figure 4 (left) and the matching shaking table displacement time history for an amplification factor (AF) of 65 % is given in Figure 4 (right).
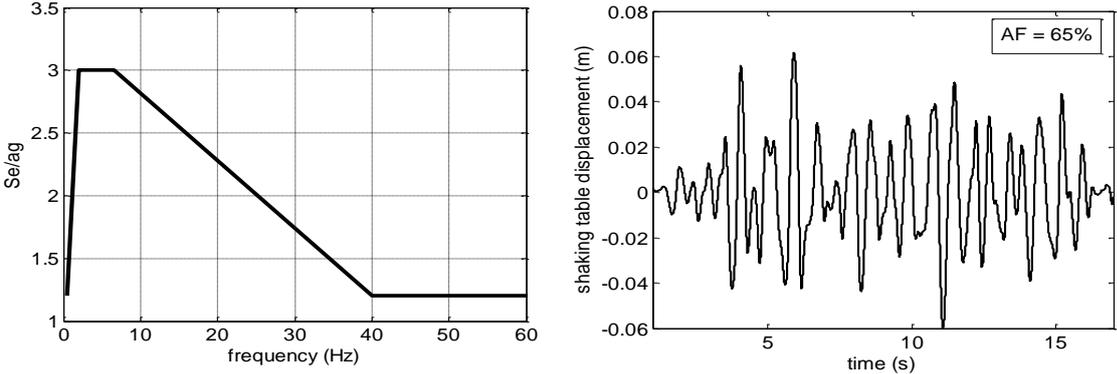

Figure 4 Design response spectrum acc. to Eurocode 8 (left) and matched shaking table displacement time history for AF=65% (right).

Amplification factors (AF) ranging from 0 to 130 % were applied to the shaking table displacement time history. Therefore, a wide range of motion inputs was employed in testing and a large set of structure response data was collected.

5

2.5 Experimental Results

The unreinforced masonry behaved elastically in the initial stage of loading and at low seismic inputs (AF less than 60%). Figure 5 (left) shows the strain energy of the URM panel during a test with AF=35%. An average quadratic potential well has been fitted for the entire time series in order to understand the pattern of mechanical behaviour. The arching in vertical plane of the uncracked panel followed an almost symmetrical pattern with slight variations caused by small translation movements and crushing of the top mortar layer against the panel frame. The angle of panel rotation went up to 2deg. When the AF reached 65%, the URM panel developed a horizontal crack at midheight along its entire width and continued arching in the vertical plane. The arching stage was associated with mechanisms of plastic deformation, with increasing out-of-plane displacements and crushing of masonry at the contact between the two rotating panel segments. The isolated peaks of strain energy are associated with masonry crushing. Figure 5 (right) shows how the panel's potential well shifts about the origin of motion as more crushing took place in higher input tests (AF=90%). The panel rotation angle increased to 5deg.
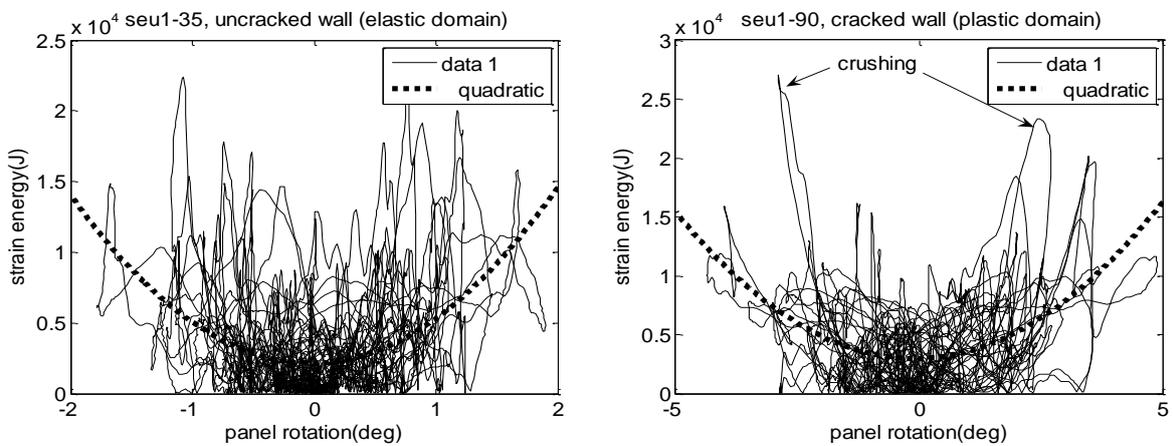

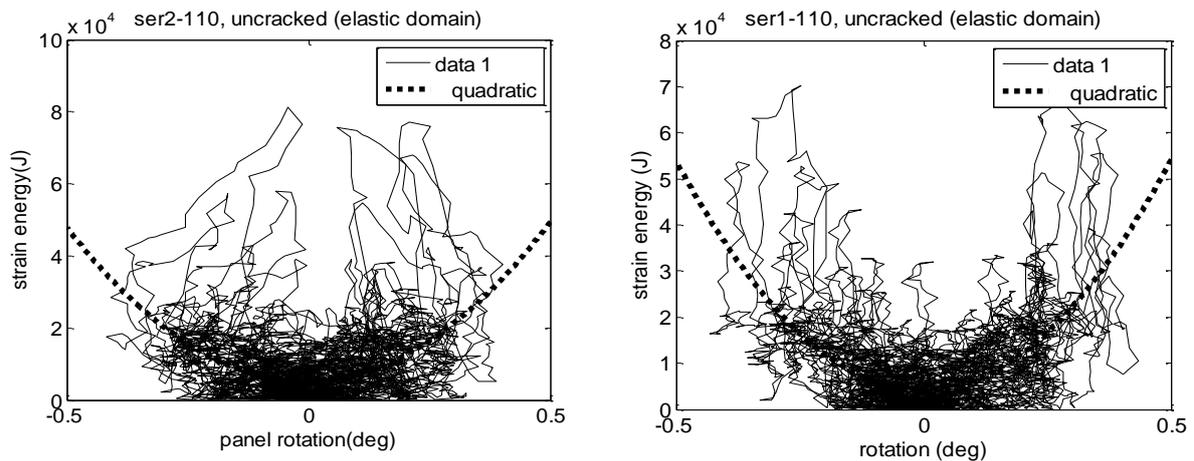Figure 5 URM panel's average potential well at AF=35% (left) and AF=90% (right).

Figure 6 Average potential well for reinforced panels
((RR=60%, AF=110% left) and (RR=100%, AF=110% right)).

By adding various amounts of reinforcement to the panels, significant changes in mechanical response took place. Higher reinforcement ratios lead to a dramatic increase of panel stiffness and natural frequency of vibration (see Table 2). The FRP reinforced panels behaved like rigid blocks and very small out-of-plane rotation angles were inferred from the displacement measurement (max 0.5deg. at

AF=110%, see Figure 6). The FRP-reinforced panels were able to withstand high accelerations without cracking. For the 40% reinforced panel (SER3 in Table 2) cracking occurred at 2.4g horizontal acceleration, while the 60% and the 100% panels remained undamaged up to 2.3g and 3.5g, respectively. These were the highest acceleration levels achievable for these particular tests so it was not possible to determine the acceleration levels at which these walls would actually start to crack. The experiments demonstrated the efficiency of the FRP systems in restricting the panel out-of-plane deformations and in preventing cracking for seismic inputs of considerable magnitude.

Table 2 Summary of results from seismic testing

Test	Reinforcement Ratio RR (%)	Uncracked natural frequency (Hz)	Cracked natural frequency (Hz)	Cracking table acceleration or max. table acceleration achieved
SEU1	0	12	7.5	cracking:1.2g(SEU1_60) collapse: 2.4g
SER1	100%	30	uncracked	max : 3.5g (SER1_130)
SER2	60%	28	uncracked	max : 2.3g (SER2_120)
SER3	40%	15	8.2	cracking: 2.4g (SEU3_80)

3. COMPUTER MODELLING

3.1 Neural Network Models

The experimental tests resulted in 64 mechanical response records for four reinforcement ratios (RR=0, RR=40%, RR=60% and RR=100%). These records were the source of training and testing for a neural network (NN) model employed in dynamic model identification. The NN model is capable of predicting the infill panel's displacement and velocity, based on its reinforcement characteristics and past response. The NN architecture features 12 inputs, 2 outputs, 3 hidden layers of 8 neurons each and 1 output layer. The NN's architecture and mode of operation were reported in Dihoru *et al* 2008. Figure 7 shows a summary diagram of the NN model: the inputs are the ground acceleration time history, the wall reinforcement ratio (RR) and the displacement and the velocity at chosen steps in time: k, $k-1$,… $k-l$; the outputs are the state variables (displacement and velocity) at step $k+1$.

An example comparison between the NN prediction and the experimentally measured state variables is shown in Figure 8. The comparison is made for a fully reinforced panel (RR=100%), subjected to a large seismic input (AF=110%).

The prediction performance of the NN model was assessed via regression analysis: the NN outputs were compared against the experimentally measured parameters in the test set. The regression analysis reveals good agreement between the NN output and the experimental values, with coefficients of regression larger than 0.9 (Figure 9).
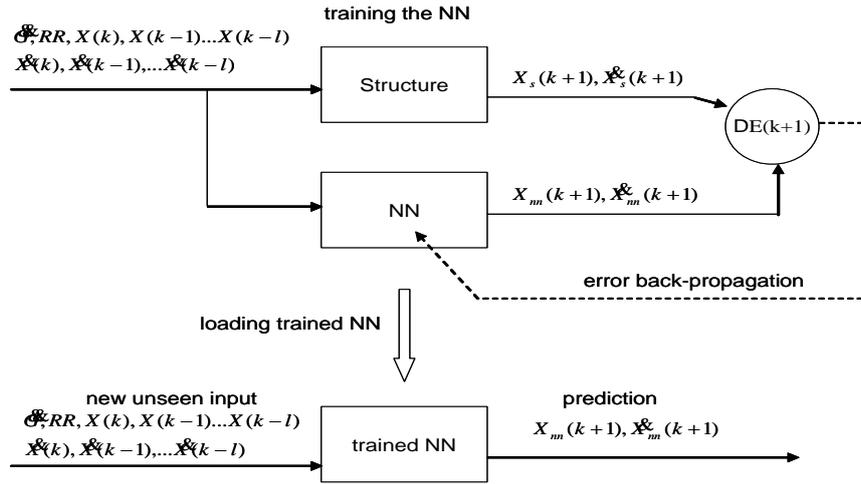
Figure 7 Neural network model for dynamic system identification: mode of operation
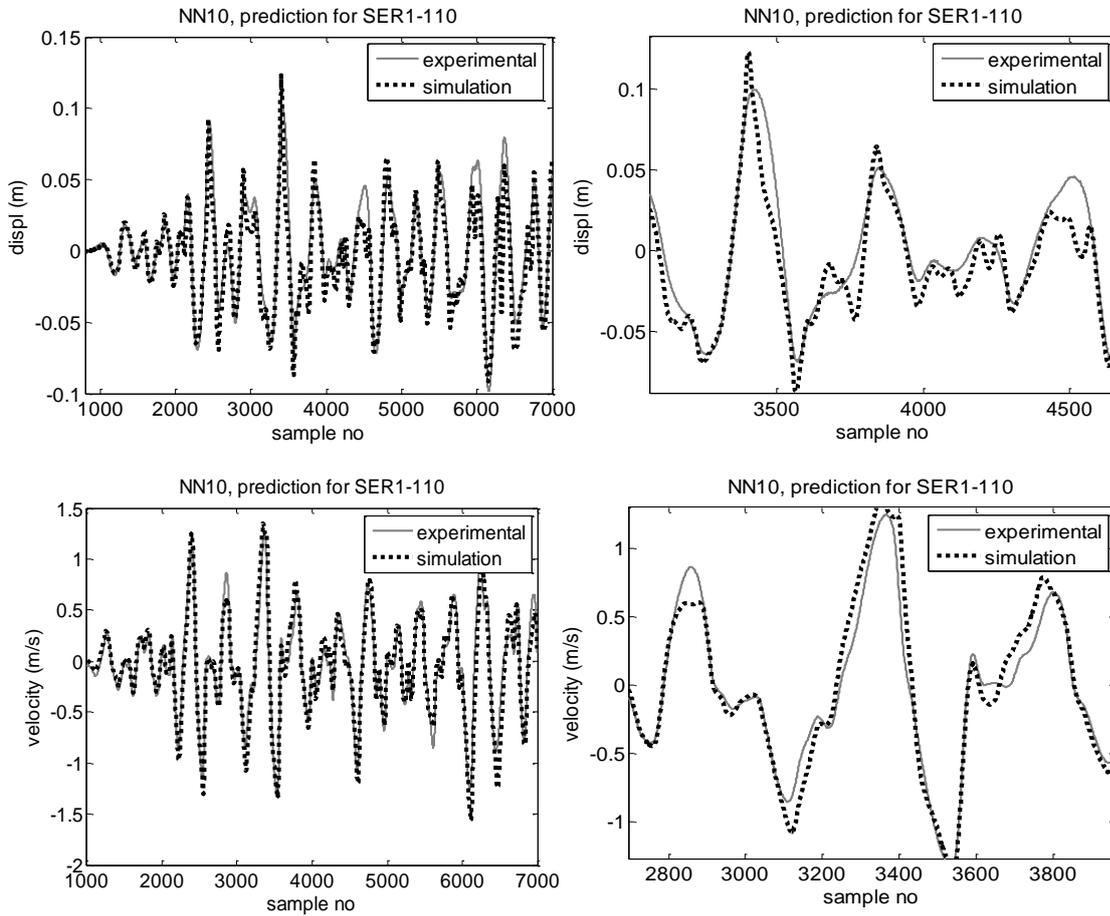

Figure 8 NN prediction and experimental measurements of out-of-plane displacement and velocity for panel SER1 (RR=100%) in test AF110%, after 20000 epochs of training.
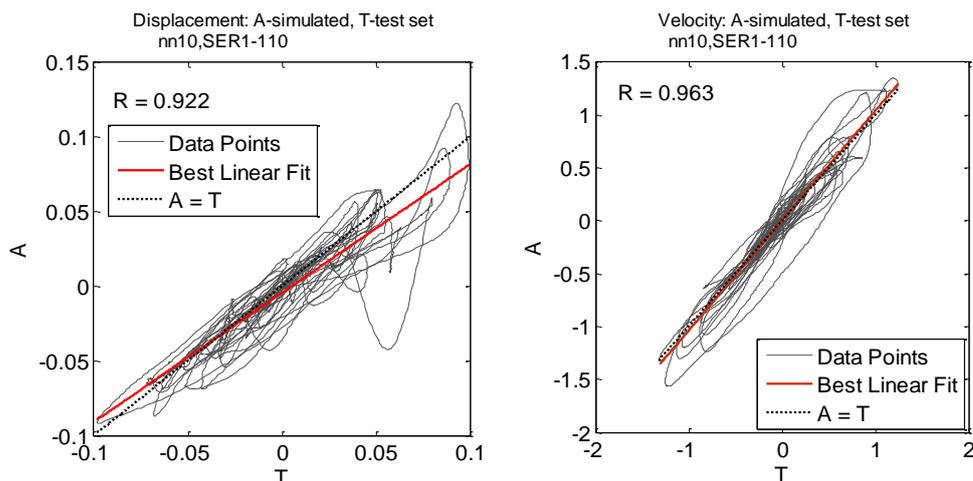
Figure 9 Regression analysis for the NN output (A) and the test set (T) for displacement, for panel SER1 (RR=100%) in test AF110% (R= regression coefficient).

The NN performance analysis demonstrated that the NN technique is a viable method for predicting the system variables when the input time history and the reinforcement ratio are known. After sufficient training, the NN can incorporate enough knowledge about the evolution of panel's stiffness and damping in order to predict the velocity and the displacement for new seismic inputs.

3.2 Discrete Element Modelling

The Discrete Element Method (DEM) was originally proposed as a numerical method for analysing the behaviour of blocky rock type systems (Cundall 1971). According to Lemos (2007), the DEM relies on the assumption that the structure being modelled can be regarded as an assembly of distinct bodies, such as masonry units, that only interact along their boundaries. The 3DEC software used in these analyses incorporates Universal Distinct Element Code (UDEC) and has been applied in many different analysis areas, such as soil and rocky systems, more recently it has also been used to model masonry (Zhen et al. 2018) and more details can be found in Itasca (2012). In 3DEC blocks can be classified as rigid or deformable. Rigid blocks do not change shape even under applied loading, while deformable blocks are sub-divided into triangular finite elements which allows calculation of deformation of the blocks. The main difference between 3DEC and a normal FE model is the fact that in 3DEC models only the blocks need to be meshed and the joints are generated automatically as additional blocks are added, as compared to FE where all the contact elements need to be specifically defined. In 3DEC, the mortar joints are built as zero-thickness interfaces and are represented by point contacts rather joint elements. These points are then used to identify the stresses and displacements across the joint.

A numerical model was built in 3DEC to investigate the out-of-plane capacity of masonry panels with a wall geometry and material properties as defined in Section 2.2 (see Figure 10). To simulate the behaviour under out-of-plane loading, first vertical gravity load was applied, then an out-of-plane horizontal acceleration was applied, in increments, until collapse occurred. The displacement of a point in the centre of the wall was monitored to develop a pushover like curve (horizontal acceleration v. horizontal displacement) to evaluate the out-of-plane capacity of the masonry panel (Figure 10b). An obvious crack appeared along the joint located about mid-height up masonry panel. In addition, some local mechanisms started to form due to failure of joints. To identify the improvement in capacity of the masonry panel with FRP-reinforcement, the numerical model was modified with the addition of a thin layer of blocks on the faces on the panel with appropriate joint properties to mimic the tensile behaviour of the FRP. The material selected for these FRP blocks was an elastic model (to increase the speed of the analysis) and the numerical models can be seen in Figures 11 and 12.

9
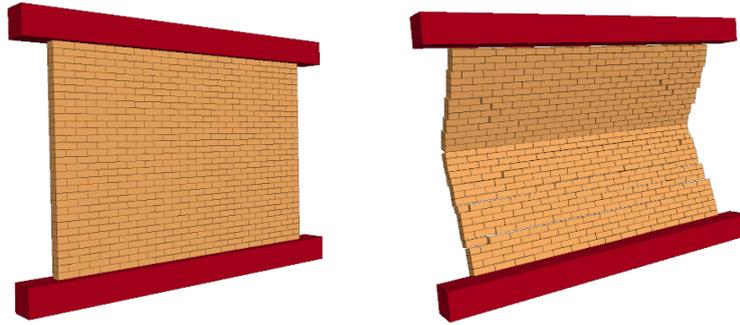
(a) Numerical model of masonry panel in 3DEC   (b) Out-of-plane failure for masonry panel

Figure 10 Numerical simulation in 3DEC for the masonry panel under out-of-plane loading.
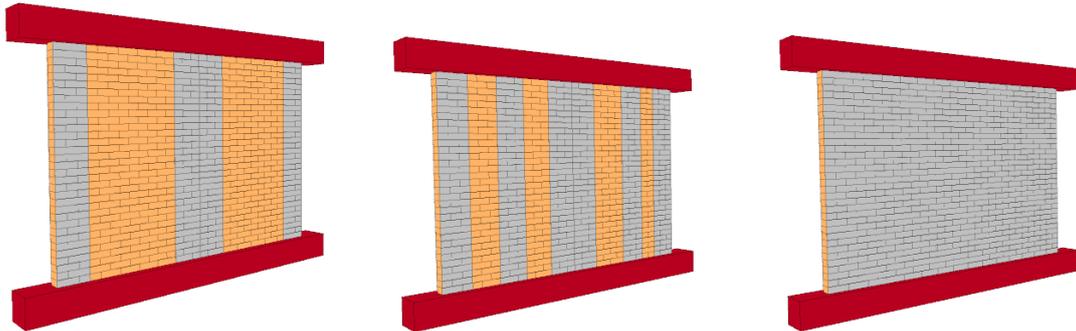

Figure 11 Layouts of FRP fabric on the numerical model. Left: vertical strips (40% RR), middle: vertical strips (60% RR), right: continuous jacket (100% RR). Reinforcement is applied on both sides of the panel. (Note: RR stands for Reinforcement Ratio).

The failure pattern and pushover curves from the analyses can be seen in Figures 12 and 13.
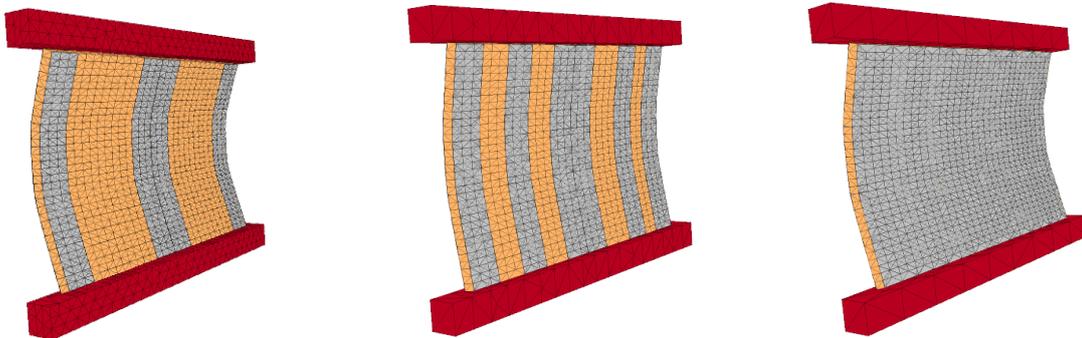

Figure 12 Failure patterns from the numerical model. Left: vertical strips (40% RR), middle: vertical strips (60% RR), right: continuous jacket (100% RR). Reinforcement is applied on both sides of the panel. (Note: RR stands for Reinforcement Ratio).

Figure 13 shows that the maximum acceleration for failure of the masonry panel with 40% RR, 60% RR and 100% RR increases by about 65%, 90% and 110% respectively compared to the masonry panel without FRP. The FRP also increases the stiffness of the panels reducing the out-of-plane displacements compared to the unreinforced wall under the same applied loading. Looking at the failure patterns from numerical models in Figure 12, it can be seen that the masonry panels with reinforcement did not show the localised horizontal cracking which the masonry panel without FRP did. The maximum acceleration at failure for the numerical model without FRP reinforcement is similar to that achieved in the experiments. Therefore, while the 3DEC modelling technique appears promising for analysing FRP reinforced masonry there was a difference predicted failure load and the experimental result for the unreinforced wall, possibly because limited material properties were available in the software so many parameters were estimated and the numerical model was simplified. For masonry panels with FRP reinforcement, the results cannot be compared directly because the experimental specimens could not be loaded to high enough values to reach failure. Nevertheless, the models confirm that masonry panels

with FRP reinforcement have a significantly improved out-of-plane capacity and localised cracking is minimised. The analyses also indicate that even a 40% RR results in a significant improvement to the panel performance.
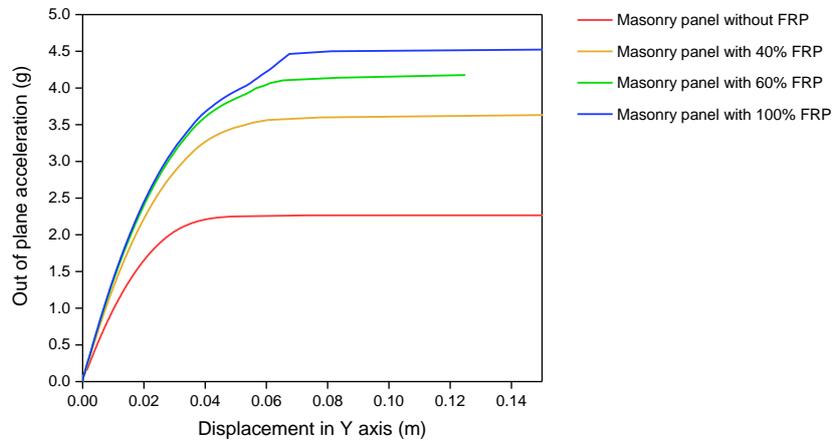

Figure 13 Pushover curves for the masonry panel with different reinforcement percentages

4. CONCLUDING REMARKS

This study has shown the efficacy of a relatively simple method of reinforcing unreinforced masonry infill panels with glass fibre FRP laminates. Provided the reinforcement covers at least 60% of the surface area of the panel (preferably 100%), and the reinforcement overlaps the surrounding frame by at least 75mm, the reinforced panel gains a significant amount of strength to out-of-plane seismic loads. So great are the strength and stiffness increases that, for typical panel configurations, it appears unlikely that a strengthened panel would suffer significant distress during an earthquake due to out-of-plane loads. For example, the 60% reinforced panel withstood accelerations of up to 2.3g without significant deformations and without cracking. The evidence derived from this study suggests that this kind of FRP strengthening can simply be specified, rather than requiring detailed engineering calculations for its justification. The method of application of the FRP reinforcement is very simple, requiring minimal training and the chosen glass fibre based materials are relatively cheap.

The NN model for dynamic system identification presented herein can forecast the panel's system variables based on past dynamic history and reinforcement data. The datasets for training can be expanded for a wider range of seismic inputs and reinforcement conditions. The advantage of any trained NN is that it can be saved and used both offline as an instrument of prediction or on-line as a control tool. This study dealt only with the off-line use of NNs, but future research may consider its use in a neuro-controller intended for real life structural systems. DEM modelling also shows promise for assessing the performance of FRP reinforced masonry wall panels. Out-of-plane analysis of the walls using 3DEC showed that FRP significantly improves the strength of masonry panels and the predicted capacity of the unreinforced wall was similar to the results obtained experimentally, although additional work still needs to be done to define more accurate material properties and numerical models for the FRP reinforcement.

5. ACKNOWLEDGEMENT

6. REFERENCES

Albert M.L., Elwi A.E., Cheng J.J.R. (2001). Strengthening of unreinforced masonry walls using FRPs, *J. Compos. for Constr.,* Vol. 5, No. 2, pp. 76-84

Bakis C.E., Bank L.C., Brown V.L., Cosenza E., Davalos J.F., Lesko J.J., Machida A., Rizkalla S.H., Triantafillou T.C. (2002). Fiber-Reinforced Polymer Composites for Construction – State-of-the-Art Review, *J. Compos. for Constr.*, Vol. 6, No. 2, pp. 73-87.

Cundall P.A (1971). A computer model for simulating progressive, large scale movement in blocky rock systems. In *Symp. ISRM, Nancy, France*, Proc 2, pp 129-136.

Dihoru, L., Taylor C.A. (2006). Deliverable 50 – Design of FRP Reinforcement of Masonry Infill Walls Against Transverse Move, *Project No.: GOCE-CT-2003-505488, LESSLOSS Risk Mitigation for Earthquakes and Landslides, Integrated Project, Sixth Framework Programme.*

Dihoru, L., Taylor C.A., Crewe A.J, Alexander N., (2008). Applications of soft computing techniques for dynamic system identification, *Proceedings of the 14th World Conference on Earthquake Engineering,* October 12-17, 2008, Beijing, China.

Ehsani M.R., Saadatmanesh H, Velasquez-Dimas, J.I. (1999). Behaviour of retrofitted URM walls under simulated earthquake loading, *J. Compos. for Constr.*, Vol. 3, No.3, pp. 134-142.

Eurocode 8: Design of Structures for Earthquake Resistance, Part 1: General Rules, Seismic Actions and Rules for Buildings, BS EN 1998-1:2004.

Hamilton H.R., Dolan C.W. (2001). Flexural Capacity of Glass FRP Strengthened Concrete Masonry Walls, *J. Compos. for Constr.*, Vol. 5, No. 3, pp. 170-178.

Gilstrap, J.M., Dolan C.W., (1998). Out-of-plane bending of FRP-reinforced masonry walls, *J. Compos. for Constr., Vol. 58, No. 8, pp. 1277-1284.*

Itasca (2012). 3DEC - Three-dimensional distinct element code. Version 5. Minneapolis, MN: Itasca Consulting Group.

Kuzic M.D., Elwi A.E., Cheng J.J.R. (2003). Cyclic flexure tests of masonry walls reinforced with glass fibre reinforced polymer sheets*, J. Compos. for Constr.*, Vol. 7, No. 1, pp. 20-30.

Lamanna A.J., Bank L.C., Scott D.W. (2001). Flexural strengthening of reinforced concrete beams using fasteners and fibre reinforced polymer strips, *ACI Struct. J.,* Vol. 98, No. 3, pp. 368-376.

Lemos J.V (2007). Discrete element modelling of masonry structures. *International Journal of Architectural Heritage*, 1(2): 190-213.

Schwegler G. (1994). Masonry construction strengthened with fibre composites in seismically endangered zones, *Proceedings of the 10th European Conf. on Earthquake Engineering,* Rotterdam, The Netherlands.

Taylor C. (1998). Seismic performance of masonry panels for Nuclear Electric plc, *EERC Project Report NE395/RP/6*, Bristol, United Kingdom.

Triantafillou T.C., Deskovic N., Deuring M. (1992). Strengthening of concrete structures with prestressed FRP sheets, *ACI Struct. J.*, Vol. 89, No. 3, pp. 235-244.

Triantafillou T.C., Fardis M.N. (1993). Advanced composites as strengthening materials of historic structures, *IABSE Symp. on Structural Preservation of the Architectural Heritage*, International Association for Bridge and Structural Engineering, Lisbon, Portugal.

Velasquez-Dimas J.I., Ehsani M.R., Saadatmanesh H. I. (2000). Out of plane behaviour of brick masonry walls strengthened with fibre composites, *ACI Struct. J.*, Vol. 97, No. 5, pp. 377-387.

Velasquez-Dimas J.I., Ehsani M.R. II, (2000). Modeling Out-of-Plane Behaviour of URM Walls Retrofitted with Fiber composites, *J. Compos. for Constr.*, Vol. 4, No.4, pp. 172-18.

Zhen L, Adam C (2018). Effect of position and size of openings on in-plane behaviour of masonry structures, *Proceedings of the 16th European Conference on Earthquake Engineering, 18-21 June, Thessaloniki, Greece.*